Seminars in Cell and Developmental Biology xxx (xxxx) xxx–xxx

Contents lists available at ScienceDirect

Seminars in Cell & Developmental Biology

journal homepage: www.elsevier.com/locate/semcdb

Review

Spatial-temporal patterning of Ca^{2+} signals by the subcellular distribution of IP_3 and IP_3 receptors

Jeffrey T. Lock[a,*], Ian F. Smith[a], Ian Parker[a,b]

[a] Department of Neurobiology & Behavior, UC Irvine, Irvine, CA, USA
[b] Department of Physiology & Biophysics, UC Irvine, Irvine, CA, USA

ARTICLE INFO

Keywords:
Image analysis
Ca^{2+} puffs
IP_3 receptors
Ca^{2+} signaling

ABSTRACT

The patterning of cytosolic Ca^{2+} signals in space and time underlies their ubiquitous ability to specifically regulate numerous cellular processes. Signals mediated by liberation of Ca^{2+} sequestered in the endoplasmic reticulum (ER) through inositol trisphosphate receptor (IP_3R) channels constitute a hierarchy of events; ranging from openings of individual IP_3 channels, through the concerted openings of several clustered IP_3Rs to generate local Ca^{2+} puffs, to global Ca^{2+} waves and oscillations that engulf the entire cell. Here, we review recent progress in elucidating how this hierarchy is shaped by an interplay between the functional gating properties of IP_3Rs and their spatial distribution within the cell. We focus in particular on the subset of IP_3Rs that are organized in stationary clusters and are endowed with the ability to preferentially liberate Ca^{2+}.

1. Introduction

Calcium is a versatile, universal, intracellular messenger. Changes in cytosolic free calcium concentrations ($[Ca^{2+}]_{cyt}$) are finely tuned by the interactions of Ca^{2+} pumps, channels and buffering proteins to serve critical roles in numerous cellular functions; controlling processes as diverse as secretion, contraction, neurotransmitter release and transcription [1,2]. The capacity to precisely and specifically regulate cellular events arises in large part through an exquisite control of the spatial and temporal patterning of $[Ca^{2+}]_{cyt}$ transients [1]. This is exemplified by the second messenger pathway mediated by inositol 1,4,5-trisphosphate (IP_3). IP_3 is generated by cleavage of membrane phosphatidylinositol bisphosphate by phospholipase C following stimulation of cell surface G-protein and tyrosine kinase coupled receptors. IP_3 then diffuses in the cytosol to bind to IP_3 receptor/channels (IP_3Rs) in the membrane of the endoplasmic reticulum (ER) that serve to liberate Ca^{2+} sequestered in the ER lumen by the activity of SERCA pumps [3]. The opening of an IP_3R channel requires not only IP_3, but also the binding of Ca^{2+} to activating sites on the cytosolic face of the tetrameric receptor [4,5]. The latter process endows IP_3-mediated signaling with a regenerative property of Ca^{2+}-induced Ca^{2+} release (CICR), because Ca^{2+} ions released from one IP_3R channel may diffuse in the cytosol and promote the opening of neighboring channels. The resulting cytosolic Ca^{2+} signals are further shaped by the clustered arrangement of IP_3Rs in the ER to generate a hierarchy of events (Fig. 1), with increasing amounts of IP_3 progressively evoking Ca^{2+} liberation from individual IP_3Rs [6] (Ca^{2+} blips), local Ca^{2+} signals arising from concerted openings of several clustered IP_3Rs [6–10] (puffs), and global Ca^{2+} elevations that engulf the cell [9,11–13].

Ca^{2+} puffs were first identified [8] and studied [6,8,10,14,15] in *Xenopus* oocytes. They have subsequently been recognized as a ubiquitous feature of Ca^{2+} signaling in numerous mammalian cell types [7,9,16–20], where they may serve local signaling functions in their own right as well as constituting the 'building blocks' for propagation of global Ca^{2+} waves, and acting as the triggers that initiate Ca^{2+} waves [9,12]. High-resolution Ca^{2+} imaging studies have revealed that puffs recur at fixed cellular sites [18,21,22] and involve the concerted openings of a few to a few tens of IP_3R channels that are clustered together within a few hundred nm [23]. The prevailing view is that the Ca^{2+} released by the stochastic opening of one channel may remain isolated to generate a blip, or may activate closely adjacent channels within a cluster by CICR to generate a puff (Fig. 1 B–D). At higher concentrations of IP_3, diffusion of Ca^{2+} over the longer distance scale (a few μm) between clusters may further propagate Ca^{2+} waves through a fire-diffuse-fire mechanism [24].

The mechanisms terminating Ca^{2+} release in the face of self-reinforcing CICR are less well understood, but are thought to involve inhibitory Ca^{2+} binding sites on the cytosolic surface on the IP_3R which

Abbreviations: $[Ca^{2+}]_{cyt}$, cytosolic free calcium concentration; CICR, Ca^{2+}-induced Ca^{2+} release; eGFP, enhanced green fluorescent protein; GPCR, G-protein-coupled receptor; IP_3, inositol 1,4,5-trisphosphate; IP_3R, inositol trisphosphate receptor; LLS, Lattice light-sheet; TIRF, total internal reflection fluorescence

* Corresponding author at: Department of Neurobiology & Behavior, University of California, Irvine, CA, 92697, USA.
E-mail address: lockj@uci.edu (J.T. Lock).

https://doi.org/10.1016/j.semcdb.2019.01.012
Received 23 October 2018; Received in revised form 17 January 2019; Accepted 22 January 2019
1084-9521/

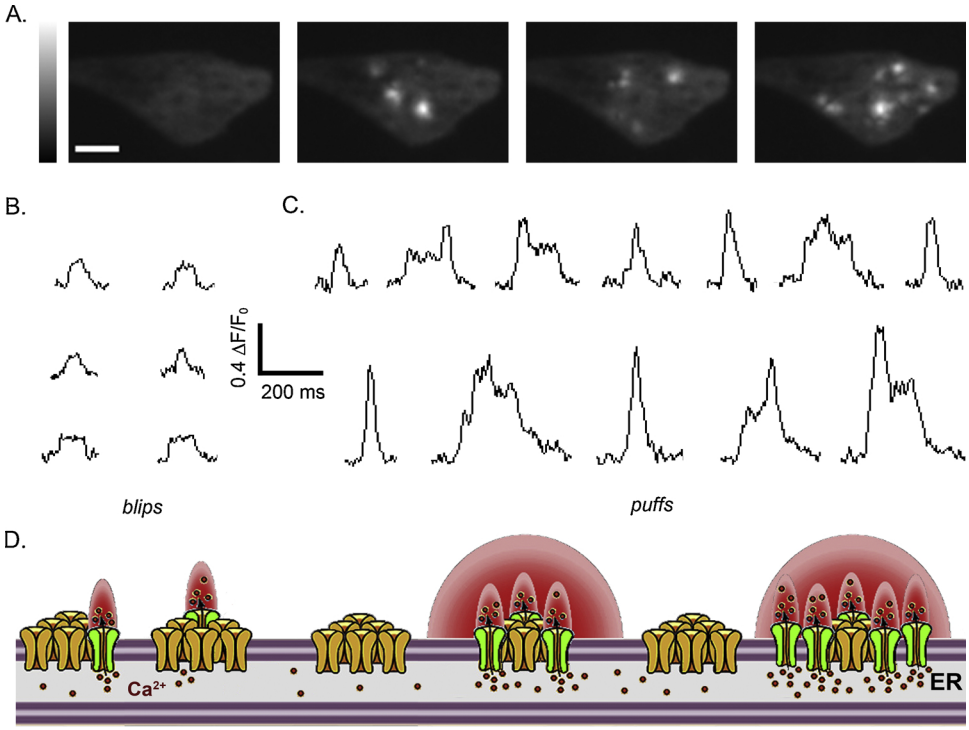

Fig. 1. The spatial-temporal patterning of local Ca^{2+} signals mediated by IP_3Rs. (A) Panels show fluorescence of a HeLa cell loaded with the Ca^{2+}-indicator Cal-520, the slow calcium buffer EGTA, and the caged IP_3 analog, i-IP_3. The first panel shows basal Cal-520 fluorescence of the cell immediately prior to the UV flash and the subsequent panels show sequential images at half second intervals following photorelease of i-IP_3. Discreet Ca^{2+} puffs can be seen arising at different times and at different sites throughout the cell. Calibration bar depicts Cal-520 fluorescence in arbitrary units from low (black) to high (white); scale bar = 20 μm. (B,C) Traces depict examples of fluorescence signals during blips (B) and puffs (C) measured from 1.5 μm^2 regions of interest placed over the centroid of each event. Scale bar indicates the change in fluorescence (ΔF) relative to the basal fluorescence (F_0) at that site before photorelease of i-IP_3. (D) Cartoon illustrating the hierarchy of IP_3R mediated local Ca^{2+} signals from blips (left) involving the activation of a single IP_3R/channel, to puffs (right) produced by the concerted opening of differing numbers of IP_3Rs within clusters.

leads to channel closure at high $[Ca^{2+}]_{cyt}$, providing an intrinsic mechanism to terminate channel activation [4,5]. Cytosolic Ca^{2+} therefore serves as both an activator and inhibitor of channel activity, a feature exemplified by the classical bell-shaped curves demonstrating the dependence of $[Ca^{2+}]$ on the open probability of IP_3Rs during electrophysiological channel recordings [4,5]. In addition to Ca^{2+}-mediated communication between IP_3Rs, observations that tightly grouped IP_3R/channels may close in a synchronized fashion suggests an additional mechanism of allosteric interaction [25], akin to the coupled-closings of ryanodine receptors [26], that ensures robust termination of Ca^{2+} release.

The spatial-temporal patterning of IP_3-mediated cytosolic Ca^{2+} signals is thus determined not only by the functional properties of IP_3Rs, but also by the subcellular spatial distribution of these receptor/channels and by the distribution of IP_3 itself. Recent progress in addressing these topics has been enhanced by advances in microscopy that enable the function, localization and motility of IP_3Rs to be examined at the single-molecule level in intact cells. We first review studies that utilize Ca^{2+} imaging as a functional reporter of IP_3R gating and localization, and then consider experiments using fluorescently-tagged IP_3Rs to determine the locations and motility of IP_3R proteins. Finally, we synthesize information derived from these functional and structural approaches in a working model wherein Ca^{2+} puffs are generated by a small number IP_3Rs that are grouped in tight clusters at fixed subcellular sites predominately located near the plasma membrane, while a majority of IP_3Rs are freely motile and appear to be functionally 'silent' under conditions that evoke puffs.

2. Imaging IP_3-mediated Ca^{2+} signals down to the single-channel level

High-resolution Ca^{2+} imaging offers a powerful means to study the activity and localization of IP_3R channels in intact cells with minimal perturbation (increased Ca^{2+} buffering by the indicator probe) of the cytoplasmic environment. As we review here, this approach provides millisecond readout of channel kinetics along with sub-micron localization of the Ca^{2+} source. Moreover, it is unbiased to the subtypes of IP_3R generating the signal, and is applicable to natively expressed IP_3Rs without needing any specific labeling of these receptors. On the other hand, drawbacks include the obvious fact that information is obtained only from those IP_3R channels that are open, and that although the location of a single open channel can be determined with high precision, blurring of the fluorescence signal by diffusion precludes the individual localization of clustered channels that open during a puff.

2.1. The 'optical patch clamp' and imaging modalities

Ca^{2+} entering the cytosol through an open IP_3R channel provides a reporter of both the gating kinetics of the channel and its location, and has the advantage of inherent amplification of the fluorescence signal because the physiological single channel Ca^{2+} current (~0.1 pA) [27] corresponds to a flux of ~10,000 Ca^{2+} ions per second, ions that may then bind to a large number of probe molecules. Advances in microscopy and fluorescent indicator dyes have made possible the imaging of such single-channel Ca^{2+} signals ('optical patch-clamp') with progressively improved resolution [28–30]. Complementing this optical approach, photorelease of a poorly metabolized IP_3 analog (i-IP_3) from a caged precursor that can readily be loaded into cells by incubation as a membrane-permeant ester [31] provides convenient control of concentration and even spatial localization of IP_3 in the cytosol [16,32].

Current generations of electron multiplied CCD and scientific CMOS cameras exhibit high sensitivity (quantum efficiency) together with superior spatial and temporal resolution, and Ca^{2+} indicator dyes that exhibit large changes in fluorescence upon binding Ca^{2+} are available in a wide range of Ca^{2+} affinities and spectral wavelengths. In conjunction with total internal reflection fluorescence (TIRF) microscopy [33], which creates an evanescent field that extends ~100 nm above the glass surface upon which cells are cultured to selective excite fluorescent cytosolic Ca^{2+} indicators adjacent to the cell membrane, these improvements have enabled the imaging of transient, subcellular changes in $[Ca^{2+}]_{cyt}$ with high fidelity [28,29]. As well as its applicability for studying plasmalemmal Ca^{2+} channels, TIRF microscopy is also optimal for studies of IP_3R channels, because the IP_3R clusters that generate puffs are, fortuitously, located in close apposition to the plasma membrane [16,18]. In contrast to spot-scanning techniques such as confocal microscopy the evanescent field permits large cell areas to

be continuously illuminated, enabling the positions and activities of many IP_3R clusters to be simultaneously imaged. Resolving the fluorescence signals produced by Ca^{2+} emanating from open IP_3R/channels can be further enhanced by loading cells with the slow Ca^{2+} buffer EGTA, which sharpens the spatial-temporal profile of puffs by limiting the diffusion of Ca^{2+} and inhibiting global elevations in $[Ca^{2+}]_{cyt}$ [34]. When imaging is then performed at high-speed acquisition rates with appropriate fluorescent reporters [35] the Ca^{2+} flux and spatial architecture of IP_3Rs can be interrogated down to the single-channel level in intact cells with a temporal resolution of ~2 ms and a spatial resolution of tens of nm. This has made it possible to determine the numbers and gating properties of the IP_3Rs underlying puffs, as well as their cellular locations [21,23,36]. In concert with advances in imaging hardware, software developed for analyzing massive data files has facilitated the automated detection, localization and analysis of local Ca^{2+} signals from multiple cells within minutes [37,38].

Light-sheet microscopy provides an alternative method for resolving time-dependent fluorescent signals, by projecting a thin sheet of excitation light through the cell and imaging the emitted fluorescence through an objective lens positioned orthogonal to the path of excitation light. An advantage of this technique is that, in contrast to TIRF microscopy, the light-sheet can be projected through any part of the cell and can be scanned to produce 3D volumetric images. Moreover, light-sheet imaging circumvents the necessity to culture cells on a glass substrate as imposed by TIRF microscopy, thereby permitting the study of cells under conditions that may more accurately reflect their native environment without sacrificing the superior spatial resolutions achieved with camera-based imaging. A recent advancement of this technique by Eric Betzig reduced the thickness of the light-sheet and extended its area by structuring it as a dithered lattice of Bessel beams [39]. Lattice light-sheet (LLS) microscopy has been applied to image Ca^{2+} puffs in SH-SY5Y cells, providing a temporal resolution and signal-to-noise ratio comparable to TIRF imaging, but extending exploration through the cell interior rather than being limited to peripheral regions immediately adjacent to the plasma membrane [40].

2.2. Imaging Ca^{2+} and dissecting Ca^{2+} puffs

TIRF imaging of local Ca^{2+} signals provides sensitivity sufficient to resolve openings of individual IP_3R channels. At some sites the fluorescence signals show a stochastic series of 'square' events of roughly constant amplitude (Fig. 1B), closely resembling electrophysiological single-channel patch-clamp records. At other sites generating larger Ca^{2+} puffs, stepwise changes in fluorescence are often apparent (Fig. 1C), which result from successive openings and closings of individual channels [23,36]. The amplitude of the unitary Ca^{2+} signal, expressed as a fluorescence ratio change ($\Delta F/F_0$), is remarkably constant (~11%) across different sites in a cell, across different cells and even between cell types [20,23,36,41,42], likely reflecting a consistent localization of IP_3R channels in close proximity to the plasma membrane [16,18,40]. Moreover, measurements of the stepwise changes in fluorescence during puffs show that these remain constant for events involving simultaneous openings of at least 5 channels [36], implying that the Ca^{2+} flux through individual channels is not appreciably reduced by local depletion of Ca^{2+} in the ER lumen even when several clustered channels are open.

2.3. Puffs arise at fixed locations, predominantly adjacent to the plasma membrane

From the earliest imaging of Ca^{2+} puffs it was evident that they arose at seemingly stationary subcellular sites, because recurrent events could be recorded from fixed, small regions of interest [8,10]. This observation was subsequently refined by using image analysis techniques to localize the centroids of puff fluorescence signals with a precision of tens of nm, indicating that the location of repeated puffs at a site remained constant within < 100 nm, even over periods of tens of minutes [18,20,43]. Localizations of Ca^{2+} blips arising from openings of individual IP_3R channels remained similarly localized [21]. We had thus concluded that individual, functional IP_3Rs, and the clusters of IP_3Rs that underlie Ca^{2+} puffs, must be anchored to some immotile, likely cytoskeletal element, rather than being freely diffusible in the membrane of the ER [22].

Although visualization of puffs by TIRF microscopy indicates that many sites of Ca^{2+} release must lie close to the plasma membrane [16,18,23], wide-field fluorescence imaging revealed further puffs that were not apparent with TIRF illumination [16], leaving open the question of whether those puffs arose in the interior of the cell, or near the plasma membrane on the 'far' side of the cell. A direct answer to this question was provided by lattice light-sheet [40] and spinning-disc confocal imaging techniques [18] that provide an optical section through the cell interior with time resolution sufficient to resolve puffs. In SH-SY5Y [40] and HeLa cells [18] puffs were found to arise almost exclusively in close proximity to the plasma membrane. This may not be a universal cellular architecture, however, as Ca^{2+} puffs in HeLa cells were previously reported to preferentially arise around the nucleus [44], and more recent findings in wild-type and gene-edited HEK-293 cells describe ~20% of puffs occurring in the cell interior [42]. Indeed, in polarized epithelial cell types such as hepatocytes [45,46] and pancreatic and parotid acinar cells [47,48] IP_3Rs are localized to specific subcellular domains within the cell interior and may not be capable of producing Ca^{2+} puffs near the plasma membrane [49].

2.4. Selective activation of puff sites by cell surface receptors?

Most studies of Ca^{2+} puffs have utilized stimulation by photorelease of IP_3 or a poorly-metabolized IP_3 analog, i-IP_3, to circumvent complications from the upstream pathway of GPCR-mediated IP_3 production and to provide better control of the magnitude, timing and spatial distribution of cytosolic $[IP_3]$ elevations [16]. IP_3 has generally been photoreleased by uniformly illuminating the cell, so that all puff sites would experience a uniform $[IP_3]$. In light of findings of hindered cytoplasmic diffusion of IP_3 [32] that raises the question of whether the puff sites activated by this procedure correspond to those natively activated by cell surface receptors that might be envisaged to deliver IP_3 selectively to specific sites. Two recent studies addressed this issue, by comparing the locations of puff sites activated in the same cell following sequential activation by extracellular application of GPCR-linked agonists and then by UV photolysis of caged i-IP_3 [20,43]. Both studies found that the two stimuli evoked puffs at the same sites, and concluded that there was no evidence that endogenous signaling pathways selectively deliver IP_3 to specific sites not accessible to photoreleased i-IP_3.

2.5. Are puff sites preformed or dynamically assembled?

Based on patch clamp recordings of excised nuclei from DT40 cells stably expressing type 1 or type 3 IP_3Rs that showed IP_3Rs to be diffusible within the lipid membrane and to rapidly (a few seconds) cluster together when $[IP_3]$ rises, it was proposed that puff sites may be dynamically assembled in response to IP_3 under physiological conditions [50]. This claim was refuted with analyses of IP_3R channel recordings by Vais H. et al. [51] and was further challenged by imaging studies on the grounds that Ca^{2+} puffs could be evoked within < 200 ms following photorelease of IP_3, a time that model simulations suggested was too brief to allow for assembly of clusters containing several IP_3Rs [22], and because stimulation of IP_3 signaling did not result in any rapid changes in motility or distribution of fluorescently tagged IP_3Rs [52]. Most recently, genetic engineering of an enhanced green fluorescent protein (eGFP) tag to native type 1 IP_3Rs has shown these to be distributed in stable punctae containing several IP_3Rs. Immobile punctae tethered close to ER-PM junctions were associated with

functional puff sites, and negligible interchange of IP_3Rs with mobile punctae was observed over many minutes [18].

2.6. Counting active IP_3Rs

Ca^{2+} imaging provides a means to estimate the number of IP_3Rs present in a cell that generate puffs. By utilizing the unitary, single IP_3R channel Ca^{2+} signal as a yardstick, the number of channels simultaneously open at the peak of a puff can be found by directly counting stepwise changes or, more readily, by dividing the peak fluorescence signal by the unitary signal. Taking this measure from the largest puff in a sequence of events then provides a minimum estimate of the number of functional IP_3Rs at the cluster underlying the puff site. Under conditions optimized to activate the maximum number of available puff sites within a cell, a rough approximation of the total number of functional IP_3Rs involved in the generation of Ca^{2+} puffs can then be calculated by taking the sum of the greatest number of IP_3Rs at each site. This is likely an underestimation however, since TIRF imaging is restricted to an ~100 nm optical section adjacent to the plasma membrane of the bottom of the cell under study, entirely neglecting or at least understating puffs originating at the top of the cell or deep within the cell interior. Although many cell types are reported to exhibit puffs almost exclusively near the plasma membrane [16,18,20], recent lattice light sheet imaging of HEK-293 cells revealed ~20% of puffs originated within the cell interior [42]. Taking all of this into account, approximations of the number of functional IP_3Rs participating in the generation of Ca^{2+} puffs range from a few hundred up to ~1000 per cell [20,22,23].

2.7. All three IP_3R isoforms mediate puffs

Vertebrates express three main IP_3R isoforms - types 1 [53], 2 [54], and 3 [55] - that are transcribed from three separate genes and co-translationally oligomerize to form tetrameric channels. These isoforms share similar monomeric molecular masses of ~300 kDa but show only 60–80% homology in their primary structures [56]. This diversity is further amplified by alternative splicing forms of these three isoforms [57–59] and because different isoforms can multimerize to form heterotetrameric channels [60–62]. Because most cell types express two or three IP_3R types [60,61,63,64], as well as a poorly defined complement of splice variants, the IP_3R population in native cells comprises a complex mixture of channel configurations with a staggering number of possible combinations [56].

Because of this diversity, the identities of the specific IP_3R isoforms underlying Ca^{2+} puffs had been difficult to resolve because all imaging studies in intact cells were performed in native cell types expressing their endogenous complement of IP_3Rs. Recently, through the use of CRISPR/Cas9 genetic engineering, the Yule lab created HEK-293 cell lines endogenously expressing single IP_3R isoforms [65]. This has facilitated investigations into the roles of IP_3R types 1, 2, and 3 in the generation of local Ca^{2+} signals, and their respective channel properties within the native cellular environment of intact cells where crucial factors including the ER membrane composition, cytosolic and ER luminal milieus are retained [27]. Using these commercially available cell lines, two studies [41,42] determined that IP_3R types 1, 2 and 3 were all capable of producing Ca^{2+} puffs in response to UV flash photolysis of i-IP_3. Puffs evoked in cells expressing each isoform remained at fixed subcellular sites, implying all three IP_3R isoforms can bind to some, as yet unidentified anchoring element/s that define the location and organization of functional IP_3R clusters. Each isoform produced puffs of similar amplitudes, single-channel Ca^{2+} fluxes and spatial distributions, although with subtle differences in puff kinetics between the different isoforms [41,42]. In contrast to their differing affinities to IP_3 observed in single-channel recordings [66], radio-ligand binding studies [54,67,68], and ER Ca^{2+} efflux assays [69], Ca^{2+} puffs displayed similar dependences on i-IP_3 concentration irrespective of the IP_3R isoform expressed [42]. Collectively, these findings demonstrate a substantial redundancy between the different IP_3R isoforms responsible for generating local Ca^{2+} signals in terms of both their channel properties and spatial distributions, suggesting that environmental and accessory factors, potentially in an isoform-specific manner, contribute to shaping unique cellular responses among different cell types.

2.8. Inferring the architecture of IP_3R clusters from Ca^{2+} imaging data

The density and spacing between IP_3Rs within the clusters underlying puff sites have important consequences for the generation of local Ca^{2+} signals, both in terms of the effectiveness of Ca^{2+} diffusion to evoke CICR from neighboring channels [36,70,71] and in light of possible allosteric interactions between IP_3Rs [25]. The 'nanoarchitecture' of the functional IP_3Rs in a cluster cannot be directly visualized from the fluorescence signal during puffs because diffusion of Ca^{2+}-bound indicator as well as the microscope point-spread signal introduce blurring greater than the expected dimensions of the cluster [70]. Nevertheless, the fluorescence signal reflects the weighted center-of-mass of those IP_3R channels open at a given time, from which useful information can be derived. Shuai et al. [72] modeled the spread of fluorescence signal expected to be generated by clusters of different dimensions, and obtained the best correspondence with experimental data suggesting that brighter puffs in *Xenopus* oocytes involved the openings of ~25 IP_3R channels, clustered within a diameter of 300–800 nm. Wiltgen et al. [21] further employed super-resolution of fluorescence signals in SH-SY5Y cells to track rapid stepwise changes in centroid position of fluorescence during individual puffs. On the assumption that these apparent movements result from asynchronous gating of different IP_3Rs, they concluded that the clusters extend over diameters of ~400 nm. Consistent with these findings, all-neighbor distance measurements of Ca^{2+} puff centroid locations in HEK WT cells and in HEK cells exclusively expressing single IP_3R types 1, 2, or 3 exhibited prominent peaks at distances < 500 nm, indicative of successive puffs recurring in close proximity, at fixed locations [42].

3. Assaying, localizing and tracking IP3R proteins

Although Ca^{2+} imaging has yielded valuable information on the subcellular distribution and localization of IP_3Rs, that technique has major limitations in that inactive IP_3R channels are invisible, and the diffusion-blurred Ca^{2+} fluorescence signal precludes mapping of multiple open channels within the clusters that underlie puffs. Accordingly, many studies have utilized a complimentary approach of fluorescently labeling IP_3R proteins, which can then be imaged at levels from macroscopic ensembles using whole-cell epifluorescence microscopy, to visualization of individual molecules by super-resolution microscopy. In most instances this has been done by overexpressing IP_3Rs tagged with a fluorescent protein, an approach that may not faithfully replicate the organization of endogenous IP_3Rs. Moreover, IP_3Rs were visualized independently of Ca^{2+} imaging, so that only inferential conclusions could be drawn regarding the relationship between the structural organization of IP_3Rs and their functional activity to liberate Ca^{2+}. Most recently, a study by Thillaipan et al. [18] mitigated these limitations, describing imaging of native type 1 IP_3Rs genetically engineered with an eGFP tag, and for the first time presenting near-simultaneous imaging of IP_3R localization together with functional imaging of Ca^{2+} puffs.

3.1. Ca^{2+} puffs are generated by a small population of immotile IP_3Rs

Radioligand binding assays indicate that typical mammalian cells contain on the order of ~7500 tetrameric IP_3Rs, corresponding to a cytoplasmic concentration of roughly 100 nM [73,74]. This number is considerably greater than the numbers of IP_3R channels (< 1000) estimated to be active in generating puffs (see section *2.6*). There is also a

marked disparity between immunostaining patterns that show IP_3Rs densely distributed throughout the entirety of the ER in mammalian cells [75–77] and observations that Ca^{2+} release arises at just a few discrete puff and blip sites [11,16,19,22,23,78,79].

Another difference arises in the immotility of IP_3Rs implied by the fixed locations of Ca^{2+} puff sites, as compared to studies of fluorescence recovery after photobleaching (FRAP) of GFP-tagged IP_3R proteins indicating that a substantial proportion of IP_3Rs are freely diffusible within the ER membrane [59,75–77,80–84], and may aggregate into clusters following sustained (minutes) activation of IP_3 signaling and/or cytosolic Ca^{2+} elevation [59,75–77,84].

Subsequent experiments have examined the motility and distribution of IP_3Rs at the single-molecule level, employing super-resolution imaging techniques to localize and track individual proteins tagged with fluorescent proteins [18,52]. Type 1 IP_3Rs tagged with mEOS and overexpressed in COS-7 cells distributed in a reticular pattern matching the ER network. Consistent with the earlier FRAP studies, a majority of the IP_3Rs (69%) were freely motile within the reticulum (diffusion coefficient D ~0.1 $\mu m^2\ s^{-1}$), whereas the remaining IP_3Rs were relatively immotile ($D < 0.008$) [52]. An ensuing study employed gene editing to tag all type 1 IP_3Rs in HeLa cells with eGFP, revealing that the IP_3Rs are distributed in punctae, each containing a few to several tetrameric IP_3Rs [18]. Super-resolved tracking of fluorescent punctae indicated that most (~70%) punctae were motile, primarily exhibiting Brownian diffusive motion, whereas the remainder appeared immotile.

To account for these apparent discrepancies in numbers, distribution and motility of IP_3Rs as monitored by functional Ca^{2+} imaging versus protein localization, we proposed that Ca^{2+} puffs arise from small numbers of IP_3Rs in immobilized clusters, whereas the majority of IP_3Rs are motile, but are functionally unresponsive ('silent') or perhaps liberate Ca^{2+} only in the presence of high concentrations of IP_3 that lead to sustained elevations of global cytosolic Ca^{2+} [22].

3.2. Silent IP_3Rs and hindered cytosolic diffusion of IP_3

What consequence might the silent majority of IP_3Rs receptors then have for cell signaling? The concentration of IP_3Rs in a typical cell (~100 nM) [85] is larger than estimates of the dissociation constant for IP_3-binding [54,68], and considerably higher than some measures of the effective concentrations of IP_3 (< 100 pM) required to evoke Ca^{2+} release [86]. Binding to silent receptors may thus be expected to buffer cytosolic concentrations of IP_3, and hinder its diffusion [32,85].

Different from this, it has been widely believed that IP_3 diffuses readily in the cytosol, with a diffusion coefficient not much slower than free diffusion in water. However, that conclusion was based on measurements of diffusion of radiolabeled IP_3 in bulk extracts of cytoplasm from *Xenopus* oocytes [24], in which the concentration of IP_3Rs was likely be much lower than in typical cells because IP_3Rs are predominantly restricted to a thin, circumferential shell underneath the plasma membrane [87]. This issue was recently reexamined by employing the latencies of Ca^{2+} puffs at different sites along the length of SH-SY5Y cells as endogenous reporters of local IP_3 concentration following photorelease of a poorly metabolized IP_3 analog at one end of the cell [32]. Fitting of the experimental data by numerical simulations yielded a diffusion coefficient ($\leq 10\ \mu m^2\ s^{-1}$) about 30-fold slower than that previously reported. Thus, in contrast to the long-accepted conclusion of Allbritton et al. [24] that IP_3 rapidly diffuses to act as a global messenger throughout cells of typical size, its hindered diffusion by binding to motile, functionally inactive receptors indicates that IP_3 is better considered a local messenger, with a range of action restricted to a few μm depending on its rate of degradation [32].

3.3. Spatial architecture of IP_3R clusters

As already noted, the density and spacing of IP_3Rs within puff sites has important consequences for how they are able to interact with each other via CICR and allosteric mechanisms. Although Ca^{2+} imaging studies indicate that IP_3Rs are spread over a few hundred nm, the resolution is insufficient to discern the nanoarchitecture of IP_3R distribution within clusters. On the other hand, super-resolution imaging techniques based on localizing the stochastic blinking of individual fluorescent proteins (PALM; [88]) or antibody-conjugated organic dyes (dSTORM; [89]) provide resolution of a few tens of nm, approaching the diameter of the IP_3R channel itself (~25 nm).

Smith et al., [52] tracked individual mEos- tagged type 1 IP_3Rs in live COS-7 cells, and identified clusters of immotile IP_3Rs situated close to the plasma membrane. The spatial distribution of IP_3Rs within these clusters varied widely, but an overlay of 70 clusters showed IP_3Rs to be distributed, on average, as an elongated oval (~400 nm on the long axis and ~200 nm on the short axis), findings that might be expected from their location along strands of the ER. Furthermore, the packing density of mEos-IP_3R molecules within clusters was highly heterogeneous. Some tight clusters exhibited IP_3R localizations within < 250 nm of each other, whilst other clusters showed a more sparse distribution.

A recent study [18], utilizing genetically engineering to tag native type 1 IP_3Rs in HeLa cells with eGFP, supports the essence of this model, while prompting important revisions. Firstly, live cell TIRF imaging of Ca^{2+} puffs in conjunction with near-simultaneous imaging of eGFP directly revealed examples of immotile IP_3R clusters underlying puff sites; although a more detailed statistical analysis is needed to substantiate this correlation and establish whether all immotile clusters are functionally active. Second, in contrast to the previous assumption that tracks of motile IP_3Rs represent individual IP_3R channels [52], a surprising finding was that motile IP_3Rs were located within punctae that moved en-mass, rather than as individual proteins [18]. By rapidly fixing cells after live TIRF imaging of eGFP punctae, STORM imaging then enabled super-resolution localization of IP_3Rs within previously identified motile and immotile punctae. Both motile and immotile punctae were found to be composed of IP_3Rs distributed across a typical area of ~0.02 μm^2, with some receptors in a cluster being closely associated whereas others were separated by distances appreciably greater than the ~25 nm size of the IP_3R itself. The authors thus proposed that IP_3Rs are corralled within mobile and immotile puncta by scaffolds that maintain a loose affiliation between IP_3Rs, without requiring their direct contact [18].

Estimates of the numbers of IP_3R channels (tetramers) within immotile clusters from single-step photobleaching and STORM imaging [18] and from single-particle tracking of over-expressed mEos-IP_3R [52] are subject to considerable uncertainties, but these approaches all point to clusters containing from a few to at most a few tens of IP_3Rs. This is in good agreement with estimates from analysis of Ca^{2+} signals, which suggest that around 2–10 IP_3R channels may open during puffs [20,36]. Thus, it seems that most, if not all IP_3Rs in the stationary clusters that underlie puff sites are functional, although the wide variability in amplitudes of successive puffs at a site indicates that only a subset of IP_3Rs may stochastically respond during any given event.

4. Summary: how the spatial organization of IP_3Rs shapes subcellular Ca^{2+} signals

Advances in imaging technology have greatly enhanced our understanding of the mechanisms underlying the generation and patterning of IP_3-mediated cellular Ca^{2+} signals. For technical reasons our knowledge derives largely from studies on immortalized cell lines (e.g. SH-SY5Y [16,19,21–23,25,32,36,40,43,90], HeLa [7,9,11,18–20,78,79], and HEK-293 cells [20,41,42]) that are readily accessible to high-resolution techniques such as TIRF microscopy. However, key attributes of Ca^{2+} puffs have been corroborated in cultures of diverse primary cell types (e.g. astrocytes [22], fibroblasts [92], endothelial cells [19], smooth muscle [93] and hippocampal neurons [94]), and cells within intact tissues (e.g. vascular endothelial cells [95] and hippocampal astrocytes

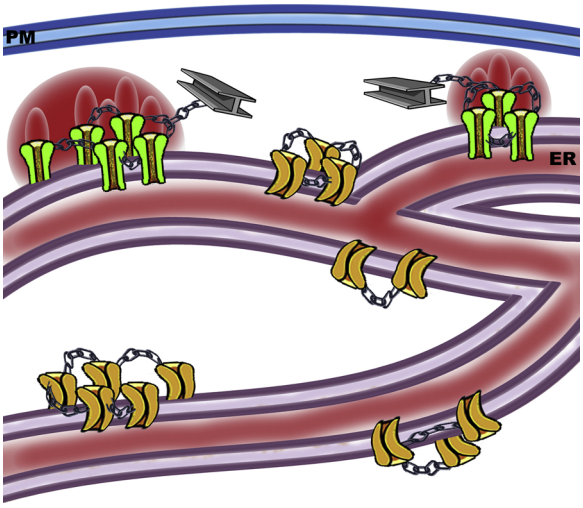

Fig. 2. Cartoon illustrating a working model of the organization and function of IP_3R clusters. Two populations IP_3R clusters are depicted: 1) A motile population of IP_3Rs (orange) that move within the endoplasmic reticulum (ER) membrane in preformed clusters with individual channels 'chained' together by an as yet unidentified scaffolding structure; and, 2) A stationary population of IP_3Rs clusters which are further held in place near the plasma membrane by 'riveting' to some cytoskeletal element. These immotile IP_3Rs are licensed to preferentially respond to low $[IP_3]$, leading to the generation of Ca^{2+} puffs at sites predominately localized close to the plasma membrane (PM).

[96]). Thus, the hierarchical organization of IP_3-mediated Ca^{2+} signals as local and global events appears ubiquitous across numerous cell types, although this architecture may be fine-tuned to suit the particular functions of specific cell types.

Fig. 2 presents a working model of how the organization and functioning of IP_3Rs may underlie the generation of local Ca^{2+} puffs at fixed subcellular sites. This is based on an earlier proposal [28], but incorporates new findings that we review here. IP_3Rs are depicted grouped within clusters; as determined for type 1 IP_3Rs [18] but yet to be confirmed for the other two IP_3R subtypes. Consistent with ensemble bleaching studies [59,75–77,80–84] and single-molecule tracking of IP_3Rs [52] a majority (~70%) of these clusters are mobile within the ER membrane, with the remainder remaining immotile over periods of at least several minutes. Little or no exchange of IP_3Rs is apparent between motile and immotile clusters, so the stationary clusters can be considered as stable entities in terms of both their localization and composition of IP_3Rs. The stationary nature of Ca^{2+} puff sites, together with the multi-channel composition of puffs, have long been taken as indicating that puffs arise from fixed clusters containing small numbers of IP_3Rs [14,23], and a recent paper [18] has correlated a mapping of puff centroids onto immotile IP_3R punctae located near the cell membrane.

Key remaining questions concern the nature of the scaffolding that assembles IP_3R in clusters and anchors them at functional puff sites. This architecture is crucial for the patterning of IP_3-mediated Ca^{2+} signaling, both in determining how IP_3Rs may interact among themselves and in placing localized Ca^{2+} signals in relation to other cellular constituents. The recent finding [18] that motile IP_3Rs do not diffuse individually throughout the ER membrane, but rather move en-mass already grouped in punctae, points to two different levels of organization; a pre-formed scaffold that defines the assembly and structure of clusters, and a second structural element, presumably associated to the cytoskeleton, that locks the clusters in place at active puff sites. These two structural elements appear to play different roles in regulating Ca^{2+} liberation through IP_3Rs. The close proximity of IP_3Rs within clusters enhances their interaction by CICR. Moreover, super-resolution imaging revealed an inhomogeneous distribution of IP_3Rs within individual clusters [18] with nm distances separating some IP_3Rs within 'sub-clusters' potentially allowing for direct protein-protein interactions that couple their gating behavior [25]. However, although IP_3R clustering leads to a greater overall channel open probability than if the same number of IP_3Rs were widely distributed [36,97] that cannot explain why puffs are almost exclusively localized to stationary punctae near the plasma membrane, because the larger number of 'silent', motile clusters have similar architecture. Thus, some unknown feature of the site to which immotile clusters bind, or the environment in which they are located, appears to 'license' those IP_3Rs so that they are preferentially able to respond at low $[IP_3]$ [18,22]. That then leaves the question of what, if any, functional role the motile clusters of IP_3Rs may play in Ca^{2+} liberation. Do they respond when strong IP_3 signaling evokes prolonged global Ca^{2+} waves and oscillations, or can the stationary sites that underlie puffs provide sufficient Ca^{2+} to elevate bulk $[Ca^{2+}]_{cyt}$ throughout the cell?

Funding

Supported by a grant from the National Institutes of HealthR37 GM048071.

Competing interests

All authors declare they have no competing interests.

Acknowledgements

We thank Dr. Angelo Demuro and Dr. Divya Swaminathan for helpful discussions concerning the measurement and analysis of local Ca^{2+} signals.

References

[1] M.J. Berridge, P. Lipp, M.D. Bootman, The versatility and universality of calcium signalling, Nat. Rev. Mol. Cell Biol. 1 (2000) 11–21, https://doi.org/10.1038/35036035.
[2] D.E. Clapham, Calcium signaling, Cell 131 (2007) 1047–1058, https://doi.org/10.1016/j.cell.2007.11.028.
[3] M.J. Berridge, Inositol trisphosphate and calcium signalling, Nature 361 (1993) 315–325, https://doi.org/10.1038/361315a0.
[4] Ilya Bezprozvanny, J. Watras, B.E. Ehrlich, Bell-shaped calcium-response curves of Ins(l,4,5)P3- and calcium-gated channels from endoplasmic reticulum of cerebellum, Nature 351 (1991) 751–754.
[5] M. Iino, Biphasic Ca2+ dependence of inositol 1,4,5-trisphosphate-induced Ca release in smooth muscle cells of the guinea pig taenia caeci, J. Gen. Physiol. 95 (1990) 1103–1122, https://doi.org/10.1085/jgp.95.6.1103.
[6] I. Parker, Y. Yao, Ca2+ transients associated with openings of inositol trisphosphate-gated channels in Xenopus oocytes, J. Physiol. 491 (1996) 663–668, https://doi.org/10.1113/jphysiol.1996.sp021247.
[7] D. Thomas, P. Lipp, S.C. Tovey, M.J. Berridge, W. Li, R.Y. Tsien, M.D. Bootman, Microscopic properties of elementary Ca2+ release sites in non-excitable cells, Curr. Biol. 10 (2000) 8–15.
[8] I. Parker, Y. Yao, Regenerative release of calcium from functionally discrete subcellular stores by inositol trisphosphate, Proc. R. Soc. B Biol. Sci. 246 (1991) 269–274, https://doi.org/10.1098/rspb.1991.0154.
[9] M.D. Bootman, M.J. Berridge, Subcellular Ca2+ signals underlying waves and graded responses in HeLa cells, Curr. Biol. 6 (1996) 855–865, https://doi.org/10.1016/S0960-9822(02)00609-7.
[10] Y. Yao, J. Choi, I. Parker, Quantal puffs of intracellular Ca2+ evoked by inositol trisphosphate in Xenopus oocytes, J. Physiol. 482 (1995) 533–553, https://doi.org/10.1113/jphysiol.1995.sp020538.
[11] M.D. Bootman, M.J. Berridge, P. Lipp, Cooking with calcium: the recipes for composing global signals from elementary events, Cell 91 (1997) 367–373, https://doi.org/10.1016/S0092-8674(00)80420-1.
[12] N. Callamaras, J.S. Marchant, X.-P. Sun, I. Parker, Activation and co-ordination of InsP3-mediated elementary Ca2+ events during global Ca2+ signals in Xenopus oocytes, J. Physiol. 509 (1998) 81–91, https://doi.org/10.1111/j.1469-7793.1998.081bo.x.
[13] J.S. Marchant, I. Parker, Role of elementary Ca2+ puffs in generating repetitive Ca2+ oscillations, EMBO J. 20 (2001) 65–76.
[14] I. Parker, J. Choi, Y. Yao, Elementary events of InsP3-induced Ca2+ liberation in Xenopus oocytes: hot spots, puffs and blips, Cell Calcium 20 (1996) 105–121, https://doi.org/10.1016/S0143-4160(96)90100-1.
[15] N. Callamaras, I. Parker, Phasic characteristic of elementary Ca(2+) release sites underlies quantal responses to IP(3), EMBO J. 19 (2000) 3608–3617, https://doi.

org/10.1093/emboj/19.14.3608.
[16] I.F. Smith, S.M. Wiltgen, I. Parker, Localization of puff sites adjacent to the plasma membrane: functional and spatial characterization of Ca2+ signaling in SH-SY5Y cells utilizing membrane-permeant caged IP3, Cell Calcium 45 (2009) 65–76, https://doi.org/10.1016/j.ceca.2008.06.001.
[17] M.L. Olson, M.E. Sandison, S. Chalmers, J.G. McCarron, Microdomains of muscarinic acetylcholine and Ins(1,4,5)P(3) receptors create “Ins(1,4,5)P(3) junctions” and sites of Ca(2)+ wave initiation in smooth muscle, J. Cell. Sci. 125 (2012) 5315–5328, https://doi.org/10.1242/jcs.105163.
[18] N.B. Thillaiappan, A.P. Chavda, S.C. Tovey, D.L. Prole, C.W. Taylor, Ca2+ signals initiate at immobile IP3 receptors adjacent to ER-plasma membrane junctions, Nat. Commun. 8 (2017) 1505, https://doi.org/10.1038/s41467-017-01644-8.
[19] S.C. Tovey, P. de Smet, P. Lipp, D. Thomas, K.W. Young, L. Missiaen, H. De Smedt, J.B. Parys, M.J. Berridge, J. Thuring, A. Holmes, M.D. Bootman, Calcium puffs are generic InsP(3)-activated elementary calcium signals and are downregulated by prolonged hormonal stimulation to inhibit cellular calcium responses, J. Cell. Sci. 114 (2001) 3979–3989.
[20] M.V. Keebler, C.W. Taylor, Endogenous signalling pathways and caged IP3 evoke Ca2+ puffs at the same abundant immobile intracellular sites, J. Cell. Sci. 130 (2017) 3728–3739, https://doi.org/10.1242/jcs.208520.
[21] S.M. Wiltgen, I.F. Smith, I. Parker, Superresolution localization of single functional IP3R channels utilizing Ca2+ flux as a readout, Biophys. J. 99 (2010) 437–446, https://doi.org/10.1016/j.bpj.2010.04.037.
[22] I.F. Smith, S.M. Wiltgen, J. Shuai, I. Parker, Ca2+ puffs originate from pre-established stable clusters of inositol trisphosphate receptors, Sci. Signal. 2 (2009), https://doi.org/10.1126/scisignal.2000466 ra77 LP-ra77.
[23] I.F. Smith, I. Parker, Imaging the quantal substructure of single IP3R channel activity during Ca2+ puffs in intact mammalian cells, Proc. Natl. Acad. Sci. U. S. A. 106 (2009) 6404–6409, https://doi.org/10.1073/pnas.0810799106.
[24] N.L. Allbritton, T. Meyer, L. Stryer, Range of messenger action of calcium-ion and inositol 1, 4, 5-trisphosphate, Science 258 (80-) (1992) 1812–1815.
[25] S.M. Wiltgen, G.D. Dickinson, D. Swaminathan, I. Parker, Termination of calcium puffs and coupled closings of inositol trisphosphate receptor channels, Cell Calcium 56 (2014) 157–168, https://doi.org/10.1016/j.ceca.2014.06.005.
[26] S.O. Marx, K. Ondrias, A.R. Marks, Coupled gating between individual skeletal muscle Ca2+release channels (ryanodine receptors), Science 281 (80-) (1998) 818–821, https://doi.org/10.1126/science.281.5378.818.
[27] D.-O.D. Mak, J.K. Foskett, Inositol 1,4,5-trisphosphate receptors in the endoplasmic reticulum: a single-channel point of view, Cell Calcium 58 (2015) 67–78, https://doi.org/10.1016/j.ceca.2014.12.008.
[28] I. Parker, I.F. Smith, Recording single-channel activity of inositol trisphosphate receptors in intact cells with a microscope, not a patch clamp, J. Gen. Physiol. 136 (2010) 119–127, https://doi.org/10.1085/jgp.200910390.
[29] A. Demuro, I. Parker, “Optical patch-clamping”: single-channel recording by imaging Ca2+ flux through individual muscle acetylcholine receptor channels, J. Gen. Physiol. 126 (2005) 179–192, https://doi.org/10.1085/jgp.200509331.
[30] A. Demuro, I. Parker, Imaging single-channel calcium microdomains, Cell Calcium 40 (2006) 413–422, https://doi.org/10.1016/j.ceca.2006.08.006.
[31] K. Dakin, W.-H. Li, Cell membrane permeable esters of d-myo-inositol 1,4,5-trisphosphate, Cell Calcium 42 (2007) 291–301, https://doi.org/10.1016/j.ceca.2006.12.003.
[32] G.D. Dickinson, K.L. Ellefsen, S. Ponce-Dawson, J.E. Pearson, I. Parker, Hindered cytoplasmic diffusion of inositol trisphosphate restricts its cellular range of action, Sci. Signal. 9 (2016).
[33] M.L. Martin-Fernandez, C.J. Tynan, S.E.D. Webb, A ‘pocket guide’ to total internal reflection fluorescence, J. Microsc. 252 (2013) 16–22, https://doi.org/10.1111/jmi.12070.
[34] S.L. Dargan, I. Parker, Buffer kinetics shape the spatiotemporal patterns of IP3-evoked Ca2+ signals, J. Physiol. 553 (2003) 775–788, https://doi.org/10.1113/jphysiol.2003.054247.
[35] J.T. Lock, I. Parker, I.F. Smith, A comparison of fluorescent Ca2+indicators for imaging local Ca2+ signals in cultured cells, Cell Calcium 58 (2015) 638–648, https://doi.org/10.1016/j.ceca.2015.10.003.
[36] G.D. Dickinson, D. Swaminathan, I. Parker, The probability of triggering calcium puffs is linearly related to the number of inositol trisphosphate receptors in a cluster, Biophys. J. 102 (2012) 1826–1836, https://doi.org/10.1016/j.bpj.2012.03.029.
[37] K.L. Ellefsen, J.T. Lock, B. Settle, C.A. Karsten, I. Parker, Applications of FLIKA, a Python-based image processing and analysis platform, for studying local events of cellular calcium signaling, Biochim. Biophys. Acta - Mol. Cell Res. (2018), https://doi.org/10.1016/j.bbamcr.2018.11.012.
[38] K.L. Ellefsen, B. Settle, I. Parker, I.F. Smith, An algorithm for automated detection, localization and measurement of local calcium signals from camera-based imaging, Cell Calcium 56 (2014) 147–156, https://doi.org/10.1016/j.ceca.2014.06.003.
[39] B.-C. Chen, W.R. Legant, K. Wang, L. Shao, D.E. Milkie, M.W. Davidson, C. Janetopoulos, X.S. Wu, J.A. Hammer, Z. Liu, B.P. English, Y. Mimori-Kiyosue, D.P. Romero, A.T. Ritter, J. Lippincott-Schwartz, L. Fritz-Laylin, R.D. Mullins, D.M. Mitchell, J.N. Bembenek, A.-C. Reymann, R. Böhme, S.W. Grill, J.T. Wang, G. Seydoux, U.S. Tulu, D.P. Kiehart, E. Betzig, Lattice light sheet microscopy: imaging molecules to embryos at high spatiotemporal resolution, Science 346 (2014) 1257998, , https://doi.org/10.1126/science.1257998.
[40] K.L. Ellefsen, I. Parker, Dynamic Ca2+ imaging with a simplified lattice light-sheet microscope: a sideways view of subcellular Ca2+ puffs, Cell Calcium 71 (2018) 34–44, https://doi.org/10.1016/j.ceca.2017.11.005.
[41] S. Mataragka, C.W. Taylor, All three IP3 receptor subtypes generate Ca2+ puffs, the universal building blocks of IP3-evoked Ca2+ signals, J. Cell. Sci. (2018), https://doi.org/10.1242/jcs.220848.
[42] J.T. Lock, K.J. Alzayady, D.I. Yule, I. Parker, All three IP3 receptor isoforms generate Ca2+ puffs that display similar characteristics, Sci. Signal. (2018), https://doi.org/10.1126/scisignal.aau0344 eaau0344.
[43] J.T. Lock, I.F. Smith, I. Parker, Comparison of Ca2+puffs evoked by extracellular agonists and photoreleased IP3, Cell Calcium 63 (2017) 43–47, https://doi.org/10.1016/j.ceca.2016.11.006.
[44] P. Lipp, D. Thomas, M.J. Berridge, M.D. Bootman, Nuclear calcium signalling by individual cytoplasmic calcium puffs, EMBO J. 16 (1997), https://doi.org/10.1093/emboj/16.23.7166 7166 LP-7173.
[45] E. Hernandez, M.F. Leite, M.T. Guerra, E.A. Kruglov, O. Bruna-Romero, M.A. Rodrigues, D.A. Gomes, F.J. Giordano, J.A. Dranoff, M.H. Nathanson, The spatial distribution of inositol 1,4,5-trisphosphate receptor isoforms shapes Ca2+ waves, J. Biol. Chem. 282 (2007) 10057–10067, https://doi.org/10.1074/jbc.M700746200.
[46] K. Hirata, T. Pusl, A.F. O’Neill, J.A. Dranoff, M.H. Nathanson, The type II inositol 1,4,5-trisphosphate receptor can trigger Ca2+ waves in rat hepatocytes, Gastroenterology 122 (2002) 1088–1100, https://doi.org/10.1053/gast.2002.32363.
[47] P. Thorn, A.M. Lawrie, P.M. Smith, D.V. Gallacher, O.H. Petersen, Local and global cytosolic Ca2+ oscillations in exocrine cells evoked by agonists and inositol trisphosphate, Cell. 74 (1993) 661–668, https://doi.org/10.1016/0092-8674(93)90513-P.
[48] J.H. Won, W.J. Cottrell, T.H. Foster, D.I. Yule, Ca2+ release dynamics in parotid and pancreatic exocrine acinar cells evoked by spatially limited flash photolysis, Am. J. Physiol. Liver Physiol. 293 (2007) G1166–G1177, https://doi.org/10.1152/ajpgi.00352.2007.
[49] J.H. Won, D.I. Yule, Measurement of Ca2+ signaling dynamics in exocrine cells with total internal reflection microscopy, Am. J. Physiol. Liver Physiol. 291 (2006) G146–G155, https://doi.org/10.1152/ajpgi.00003.2006.
[50] A. Taufiq-Ur-Rahman, M. Skupin, C.W. Falcke, Taylor, Clustering of InsP3 receptors by InsP3 retunes their regulation by InsP3 and Ca2+, Nature 458 (2009) 655–659, https://doi.org/10.1038/nature07763.
[51] H. Vais, J.K. Foskett, D.-O.D. Mak, InsP3R channel gating altered by clustering? Nature 478 (2011) E1, https://doi.org/10.1038/nature10493.
[52] I.F. Smith, D. Swaminathan, G.D. Dickinson, I. Parker, Single-molecule tracking of inositol trisphosphate receptors reveals different motilities and distributions, Biophys. J. 107 (2014) 834–845, https://doi.org/10.1016/j.bpj.2014.05.051.
[53] T. Furuichi, S. Yoshikawa, A. Miyawaki, K. Wada, N. Maeda, K. Mikoshiba, Primary structure and functional expression of the inositol 1,4,5-trisphosphate-binding protein P400, Nature 342 (1989) 32–38, https://doi.org/10.1038/342032a0.
[54] T.C. Südhof, C.L. Newton, B.T. Archer, Y.A. Ushkaryov, G.A. Mignery, Structure of a novel InsP3 receptor, EMBO J. 10 (1991) 3199–3206 http://www.ncbi.nlm.nih.gov/pmc/articles/PMC453043/.
[55] O. Blondel, J. Takeda, H. Janssen, S. Seino, G.I. Bell, Sequence and functional characterization of a third inositol trisphosphate receptor subtype, IP3R-3, expressed in pancreatic islets, kidney, gastrointestinal tract, and other tissues, J. Biol. Chem. 268 (1993) 11356–11363 http://www.jbc.org/content/268/15/11356.abstract.
[56] J.K. Foskett, C. White, K.-H. Cheung, D.-O.D. Mak, Inositol Trisphosphate Receptor Ca2+ Release Channels, Physiol. Rev. 87 (2007) 593–658, https://doi.org/10.1152/physrev.00035.2006.
[57] S.K. Danoff, C.D. Ferris, C. Donath, G.A. Fischer, S. Munemitsu, A. Ullrich, S.H. Snyder, C.A. Ross, Inositol 1,4,5-trisphosphate receptors: distinct neuronal and nonneuronal forms derived by alternative splicing differ in phosphorylation, Proc. Natl. Acad. Sci. 88 (1991) 2951–2955, https://doi.org/10.1073/pnas.88.7.2951.
[58] T. Nakagawa, H. Okano, T. Furuichi, J. Aruga, K. Mikoshiba, The subtypes of the mouse inositol 1,4,5-trisphosphate receptor are expressed in a tissue-specific and developmentally specific manner, Proc. Natl. Acad. Sci. 88 (1991) 6244–6248 http://www.pnas.org/content/88/14/6244.abstract.
[59] M. Iwai, Y. Tateishi, M. Hattori, A. Mizutani, T. Nakamura, A. Futatsugi, T. Inoue, T. Furuichi, T. Michikawa, K. Mikoshiba, Molecular cloning of mouse type 2 and type 3 inositol 1,4,5-Trisphosphate receptors and identification of a novel type 2 receptor splice variant, J. Biol. Chem. 280 (2005) 10305–10317, https://doi.org/10.1074/jbc.M413824200.
[60] T. Monkawa, A. Miyawaki, T. Sugiyama, H. Yoneshima, M. Yamamoto-Hino, T. Furuichi, T. Saruta, M. Hasegawa, K. Mikoshiba, Heterotetrameric complex formation of inositol 1,4,5-Trisphosphate receptor subunits, J. Biol. Chem. 270 (1995) 14700–14704, https://doi.org/10.1074/jbc.270.24.14700.
[61] R.J.H. Wojcikiewicz, Y.Q. He, Type-I, Type-II and Type-III inositol 1,4,5-Trisphosphate receptor Co-immunoprecipitation as evidence for the existence of heterotetrameric receptor complexes, Biochem. Biophys. Res. Commun. 213 (1995) 334–341, https://doi.org/10.1006/bbrc.1995.2134.
[62] S.K. Joseph, C. Lin, S. Pierson, A.P. Thomas, A.R. Maranto, Heteroligomers of Type-I and Type-III inositol trisphosphate receptors in WB rat liver epithelial cells, J. Biol. Chem. 270 (1995) 23310–23316, https://doi.org/10.1074/jbc.270.40.23310.
[63] T.H. Grayson, R.E. Haddock, T.P. Murray, R.J.H. Wojcikiewicz, C.E. Hill, Inositol 1,4,5-trisphosphate receptor subtypes are differentially distributed between smooth muscle and endothelial layers of rat arteries, Cell Calcium 36 (2004) 447–458, https://doi.org/10.1016/j.ceca.2004.04.005.
[64] D.I. Yule, S.A. Ernst, H. Ohnishi, R.J.H. Wojcikiewicz, Evidence that zymogen granules are not a physiologically relevant calcium pool: defining the distribution of inositol 1,4,5-trisphosphate receptors in pancreatic acinar cells, J. Biol. Chem. 272 (1997) 9093–9098, https://doi.org/10.1074/jbc.272.14.9093.
[65] K.J. Alzayady, L. Wang, R. Chandrasekhar, L.E.W. Ii, F. Van Petegem, D.I. Yule, Defining the stoichiometry of inositol 1, 4, 5-trisphosphate binding required to

initiate Ca 2 + release, Sci. Signal. 9 (2016) 1–12 http://stke.sciencemag.org/content/9/422/ra35.abstract.
[66] H. Tu, Z. Wang, E. Nosyreva, H. De Smedt, I. Bezprozvanny, Functional characterization of mammalian inositol 1,4,5-Trisphosphate receptor isoforms, Biophys. J. 88 (2005) 1046–1055, https://doi.org/10.1529/biophysj.104.049593.
[67] R.J. Wojcikiewicz, S.G. Luo, Differences among type I, II, and III inositol-1,4,5-trisphosphate receptors in ligand-binding affinity influence the sensitivity of calcium stores to inositol-1,4,5-trisphosphate, Mol. Pharmacol. 53 (1998) 656–662, https://doi.org/10.1124/mol.53.4.656.
[68] C.L. Newton, G.A. Mignery, T.C. Südhof, Co-expression in vertebrate tissues and cell lines of multiple inositol 1,4,5-trisphosphate (InsP3) receptors with distinct affinities for InsP3, J. Biol. Chem. 269 (1994) 28613–28619 http://www.jbc.org/content/269/46/28613.abstract.
[69] T. Miyakawa, a Maeda, T. Yamazawa, K. Hirose, T. Kurosaki, M. Iino, Encoding of Ca2+ signals by differential expression of IP3 receptor subtypes, EMBO J. 18 (1999) 1303–1308, https://doi.org/10.1093/emboj/18.5.1303.
[70] J. Shuai, I. Parker, Optical single-channel recording by imaging Ca2+ flux through individual ion channels: theoretical considerations and limits to resolution, Cell Calcium 37 (2005) 283–299, https://doi.org/10.1016/j.ceca.2004.10.008.
[71] J. Shuai, J.E. Pearson, J.K. Foskett, D.-O.D. Mak, I. Parker, A kinetic model of single and clustered IP3 receptors in the absence of Ca2+ feedback, Biophys. J. 93 (2007) 1151–1162, https://doi.org/10.1529/biophysj.107.108795.
[72] J. Shuai, H.J. Rose, I. Parker, The number and spatial distribution of IP3 receptors underlying calcium puffs in Xenopus oocytes, Biophys. J. 91 (2006) 4033–4044, https://doi.org/10.1529/biophysj.106.088880.
[73] C.W. Taylor, V. Konieczny, IP3 receptors: take four IP3 to open, Sci. Signal. 9 (2016) pe1 LP-pe1 http://stke.sciencemag.org/content/9/422/pe1.abstract.
[74] S.C. Tovey, S.G. Dedos, E.J.A. Taylor, J.E. Church, C.W. Taylor, Selective coupling of type 6 adenylyl cyclase with type 2 IP3 receptors mediates direct sensitization of IP3 receptors by cAMP, J. Cell Biol. 183 (2008) 297–311, https://doi.org/10.1083/jcb.200803172.
[75] M. Chalmers, M.J. Schell, P. Thorn, Agonist-evoked inositol trisphosphate receptor (IP3R) clustering is not dependent on changes in the structure of the endoplasmic reticulum, Biochem. J. 394 (2006) 57–66, https://doi.org/10.1042/BJ20051130.
[76] Y. Tateishi, M. Hattori, T. Nakayama, M. Iwai, H. Bannai, T. Nakamura, T. Michikawa, T. Inoue, K. Mikoshiba, Cluster formation of inositol 1,4,5-Trisphosphate receptor requires its transition to open state, J. Biol. Chem. 280 (2005) 6816–6822, https://doi.org/10.1074/jbc.M405469200.
[77] B.S. Wilson, J.R. Pfeiffer, A.J. Smith, J.M. Oliver, J.A. Oberdorf, R.J.H. Wojcikiewicz, Calcium-dependent clustering of inositol 1,4,5-Trisphosphate receptors, Mol. Biol. Cell 9 (1998) 1465–1478 http://www.ncbi.nlm.nih.gov/pmc/articles/PMC25370/.
[78] D. Thomas, P. Lipp, M.J. Berridge, M.D. Bootman, Hormone-evoked elementary Ca2+ signals are not stereotypic, but reflect activation of different size channel clusters and variable recruitment of channels within a cluster, J. Biol. Chem. 273 (1998) 27130–27136, https://doi.org/10.1074/jbc.273.42.27130.
[79] M. Bootman, E. Niggli, M. Berridge, P. Lipp, Imaging the hierarchical Ca2+ signalling system in HeLa cells, J. Physiol. 499 (1997) 307–314 http://www.ncbi.nlm.nih.gov/pmc/articles/PMC1159306/.
[80] C. Cruttwell, J. Bernard, M. Hilly, V. Nicolas, R.E.A. Tunwell, J.-P. Mauger, Dynamics of the Ins(1,4,5)P3 receptor during polarization of MDCK cells, Biol. Cell 97 (2012) 699–707, https://doi.org/10.1042/BC20040503.
[81] M. Ferreri-Jacobia, D.-O.D. Mak, J.K. Foskett, Translational mobility of the type 3 inositol 1,4,5-Trisphosphate receptor Ca2+ release channel in endoplasmic reticulum membrane, J. Biol. Chem. 280 (2005) 3824–3831, https://doi.org/10.1074/jbc.M409462200.
[82] K. Fukatsu, H. Bannai, S. Zhang, H. Nakamura, T. Inoue, K. Mikoshiba, Lateral diffusion of inositol 1,4,5-Trisphosphate receptor type 1 is regulated by actin filaments and 4.1N in neuronal dendrites, J. Biol. Chem. 279 (2004) 48976–48982, https://doi.org/10.1074/jbc.M408364200.
[83] C.J. Gibson, B.E. Ehrlich, Inositol 1,4,5-trisphosphate receptor movement is restricted by addition of elevated levels of O-linked sugar, Cell Calcium 43 (2008) 228–235, https://doi.org/10.1016/j.ceca.2007.05.008.
[84] Y. Tojyo, T. Morita, A. Nezu, A. Tanimura, The clustering of inositol 1,4,5-trisphosphate (IP3) receptors is triggered by IP3 binding and facilitated by depletion of the Ca2+ store, J. Pharmacol. Sci. 107 (2008) 138–150, https://doi.org/10.1254/jphs.08021FP.
[85] C.W. Taylor, V. Konieczny, IP3 receptors: take four IP3 to open, Sci. Signal. 9 (2016), https://doi.org/10.1126/scisignal.aaf6029 pe1-pe1.
[86] A. Demuro, I. Parker, Picomolar sensitivity to inositol trisphosphate in Xenopus oocytes, Cell Calcium 58 (2015) 511–517, https://doi.org/10.1016/j.ceca.2015.08.003.
[87] N. Callamaras, I. Parker, Radial localization of inositol 1,4,5-Trisphosphate–sensitive Ca2+ release sites in Xenopus oocytes resolved by axial confocal linescan imaging, J. Gen. Physiol. 113 (1999) 199–213 http://www.ncbi.nlm.nih.gov/pmc/articles/PMC2223371/.
[88] E. Betzig, G.H. Patterson, R. Sougrat, O.W. Lindwasser, S. Olenych, J.S. Bonifacino, M.W. Davidson, J. Lippincott-Schwartz, H.F. Hess, Imaging intracellular fluorescent proteins at nanometer resolution, Science 313 (80-) (2006) 1642 LP-1645 http://science.sciencemag.org/content/313/5793/1642.abstract.
[89] M. Heilemann, S. van de Linde, M. Schüttpelz, R. Kasper, B. Seefeldt, A. Mukherjee, P. Tinnefeld, M. Sauer, Subdiffraction-Resolution Fluorescence Imaging with Conventional Fluorescent Probes, Angew. Chemie Int. Ed. 47 (n.d.) 6172–6176. doi:https://doi.org/10.1002/anie.200802376.
[90] G.D. Dickinson, I. Parker, Factors determining the recruitment of inositol trisphosphate receptor channels during calcium puffs, Biophys. J. 105 (2013) 2474–2484, https://doi.org/10.1016/j.bpj.2013.10.028.
[92] G. Schmunk, B.J. Boubion, I.F. Smith, I. Parker, J.J. Gargus, Shared functional defect in IP_3R-mediated calcium signaling in diverse monogenic autism syndromes, Transl. Psychiatry 5 (2015), https://doi.org/10.1038/tp.2015.123 e643–e643.
[93] V.A. Miriel, J.R. Mauban, M.P. Blaustein, W.G. Wier, Local and cellular Ca2+ transients in smooth muscle of pressurized rat resistance arteries during myogenic and agonist stimulation, J. Physiol. (Paris) 518 (Pt 3) (1999) 815–824, https://doi.org/10.1111/j.1469-7793.1999.0815p.x.
[94] S. Koizumi, M.D. Bootman, L.K. Bobanović, M.J. Schell, M.J. Berridge, P. Lipp, Characterization of Elementary Ca2+ Release Signals in NGF-Differentiated PC12 Cells and Hippocampal Neurons, Neuron 22 (1999) 125–137, https://doi.org/10.1016/S0896-6273(00)80684-4.
[95] J. Ledoux, M.S. Taylor, A.D. Bonev, R.M. Hannah, V. Solodushko, B. Shui, Y. Tallini, M.I. Kotlikoff, M.T. Nelson, Functional architecture of inositol 1,4,5-trisphosphate signaling in restricted spaces of myoendothelial projections, Proc. Natl. Acad. Sci. U. S. A. 105 (2008) 9627–9632, https://doi.org/10.1073/pnas.0801963105.
[96] M.W. Sherwood, M. Arizono, C. Hisatsune, H. Bannai, E. Ebisui, J.L. Sherwood, A. Panatier, S.H.R. Oliet, K. Mikoshiba, Astrocytic IP3Rs: contribution to Ca2+ signalling and hippocampal LTP, Glia. 65 (2017) 502–513, https://doi.org/10.1002/glia.23107.
[97] J.W. Shuai, P. Jung, Optimal ion channel clustering for intracellular calcium signaling, Proc. Natl. Acad. Sci. 100 (2003) 506–LP-510 http://www.pnas.org/content/100/2/506.abstract.